Scientia Iranica B (2021) 28(2), 721–730

Sharif University of Technology
Scientia Iranica
Transactions B: Mechanical Engineering
http://scientiairanica.sharif.edu

Investigating the second law of thermodynamics and three-dimensional flow study within the vortex tube device using computational fluid dynamics

N. Pourmahmoud* **and O. Moutaby**

Department of Mechanical Engineering, Urmia University, Urmia, Iran.

Received 21 June 2018; received in revised form 5 October 2018; accepted 8 December 2018

KEYWORDS
Vortex tube;
Inlet pressure;
Energy separation;
Mach number;
Exergy.

Abstract. In this paper, the effect of inlet pressure on the performance of a vortex tube device is investigated using Three-Dimensional (3D) simulation and Computational Fluid Dynamics (CFD) technique by fluent software. The flow inside the device is considered to be compressible and turbulent. In order to understand and investigate the effect of inlet pressure, different inlet pressures are added to the device, and the results are extracted and analyzed. The main objective of this study is to achieve a minimum cold exit temperature and maximum swirl velocity in the vortex tube. This paper demonstrates that an inlet pressure of 4.8 bars is an optimal inlet pressure, which is justifiable in terms of economy and the amount of produced cooling. The CFD results show that an increase in inlet pressure leads to an increase in the entropy production and, subsequently, the system disorder. Finally, the existing gaps in the previous studies will be filled by examining the inlet and exit exergies in the vortex tube device. Inlet exergy has not made considerable changes in terms of α and has a constant value. In addition, at $\alpha = 0.3691$, the minimum exergy efficiency occurs according to the calculations.

1. Introduction

The vortex tube or Ranque-Hilsch vortex tube is a mechanical device with relatively ordinary geometry and without any complexities in the number of components, which can convert the compressed inlet air into two separate hot and cold parts [1]. The vortex tube divides the input gas flow to the tube into two separate flows: One is warmer and the other is cooler than the input flow. A remarkable note about this device is the absence of any moving parts, electrical or chemical components, or input power to it. Despite the simplicity of vortex tube geometry, its fluid dynamic process and thermodynamics can be very complex [2].

Many laboratory, theoretical, and numerical studies have been carried out to investigate the temperature separation phenomenon in the vortex tube so far. Clearly, the application of the Computational Fluid Dynamics (CFD) technique reduces the complexity and cost of empirical works [3-7]. Figure 1 shows the operation of a vortex tube with its components.

The vortex tube was accidentally discovered in 1930 by a French physics student named George Ranque [9]. Following him, Rudolf Hilsch [10], a German physicist, began studying the vortex tube throughout a paper.

With the advent of computers and their entry into the field of science and the expansion of the use of numerical methods, the use of CFD techniques has expanded more than ever among researchers in the

*. *Corresponding author.*
E-mail addresses: n.pormahmod@urmia.ac.ir (N. Pourmahmoud); o.moutaby@urmia.ac.ir (O. Moutaby)

doi: 10.24200/sci.2018.51263.2086

Figure 1. Vortex tube device and its operation [8].

field of vortex tube. The application of numerical studies reduces the complexity of laboratory works, in addition to the attractiveness of the subject, and greatly helps understand the physics of the flow and the problem [11,12]. Extensive works have been done in this field. The following are some of the most important numerical studies that are relevant to the subject of this paper.

Behera et al. [14] performed the most comprehensive numerical research on the shape of the profile and the number of nozzles. According to the results of their research, the vortex tube with 6 convergent injection nozzles has the best performance and makes the highest temperature separation due to the proper radial symmetry of the flow field inside the vortex chamber and high swirl velocity achievement. In 2010, Shamsoddini and HosseinNezhad [15] numerically investigated the effect of the number of nozzles. They showed that an increase in the number of nozzles increased the cooling power, which corresponded to a decrease in cold exit temperature; however, this increase is negligible.

In 2014, Pourmahmoud et al. [16] numerically investigated the effect of the geometric nozzle parameter on the energy separation. According to their results, increasing the outlet pressures of nozzles' hole value enhanced the machine's cooling capacity in most operating conditions. In 2015, Pourmahmoud et al. [17] examined the effect of length on the location of the stagnation point. They investigated the location of stagnation point along the tube on temperature separation in the vortex tube using a numerical model with different lengths. They concluded that the location of the stagnation point was closer to the hot exit at a length of 106 mm in comparison with other models, and this model produced the highest temperature difference between the cold and hot exits.

In general, the number of published numerical articles in the field of inlet pressure in the vortex tube is negligible. Ameri and Behnia [18] conducted one of the CFD works in this field. They showed that an increase in inlet pressure increased the efficiency of the vortex tube; however, from 6 bars, an increase in inlet pressure decreased the efficiency. Zhidkov et al. [19], Skye et al. [20], and Pourmahmoud et al. [21] concluded that an increase in pressure increased ΔT_{ic}.

No satisfactory theory has been presented to explain the temperature separation phenomenon in the vortex tube so far. Some researchers have attributed energy separation to the transfer of work along with compression and expansion, and others have proposed the effect of turbulent vortices. The secondary rotation has been expressed as another factor in energy separation. The items mentioned above (often a large range of inlet pressures) and only the cold and hot exit temperatures have been considered as parameters. However, this study attempts to reduce the intervals between the inlet pressure values and investigate additional parameters such as swirl velocity and Mach number. In addition, the innovation of the present work lies in considering the Mach number inside the 4vortex chamber and its variations due to the changes in the inlet pressure, which has not been studied in other papers so far. Besides, one can find new results in the area of inlet and outlet exergies through the vortex tube machine.

2. Numerical model and governing equations

The numerical model is based on a model presented by Skye et al. [20]. This model is equipped with six air inlet nozzles and hot and cold exits. Figure 2 shows the geometry of the problem. The exact geometric dimensions of the modeled vortex tube are presented in Table 1.

The numerical model of the vortex tube has been simulated by fluent software package. The fundamental

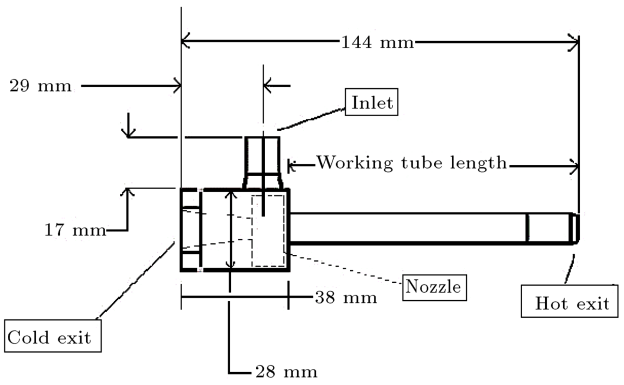

Figure 2. Schematic outline of the examined vortex tube and its dimensions [20].

Table 1. Geometric dimensions of the modeled vortex tube.

Parameter	Value
Length of tube	106 mm
Diameter of tube	4.11 mm
Depth of nozzle	0.97 mm
Width of nozzle	1.41 mm
Total area of nozzle's inlet	8.2 mm^2
Diameter of cold exit	6.2 mm
Diameter of hot exit	11 mm

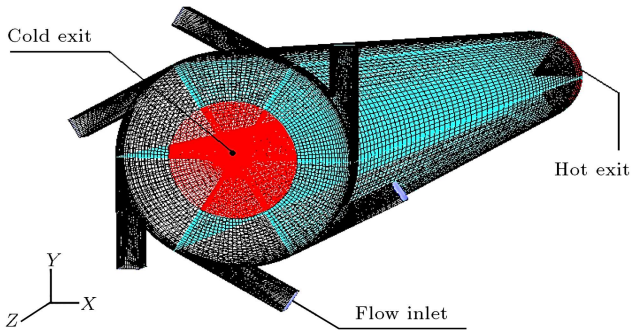

Figure 3. The meshing profile of 3D model by displaying the computational field of problem.

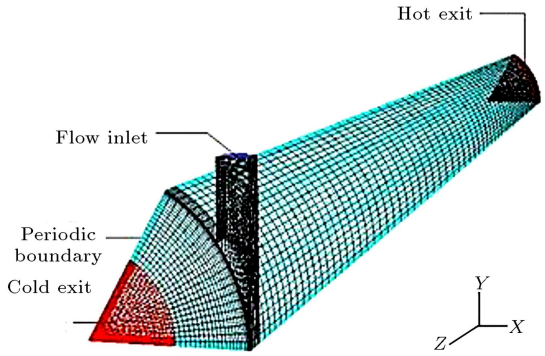

Figure 4. The meshing profile of 3D model by displaying the computational field of the problem.

equations have been solved using the code of this software in a 3D compressible and turbulent field.

Structured mesh elements have been used for the meshing of 3D model. Figure 3 shows the generated mesh for the considered 3D model.

Due to the presence of a high gradient at the inlet and exits, finer grids have been used in these areas, which are evident in the figure. Further, due to the periodic shape of the vortex tube, only $\frac{1}{6}$ of the total shape has been modeled to reduce the volume of calculations and shorten the execution time of the program, as shown in Figure 4.

Considering that the flow in the vortex tube is highly turbulent, a turbulence model must be used to consider the turbulence effect besides the conservation of mass, momentum, and energy and gas state equations for the numerical modeling of compressible flow in the vortex tube.

The governing equations for the 3D flow field include conservation of mass, momentum, and energy and gas state equations.

In addition to the above equations, the equations related to the $k-\varepsilon$ turbulence model must be solved simultaneously. These equations can be found in detail in [4,5]. Thus, they are not shown here for abbreviations.

The assumptions used in this research are as follows:

1. The flow is compressible;
2. The operating fluid is air;
3. The flow within the vortex tube is highly turbulent;
4. The geometric parameters of the tube such as length, diameter, and nozzle dimensions are constant.

The finite volume method is applied by the fluent software to a 3D mesh, shown in Figure 4, along with the boundary conditions expressed in the next section. The second-order upwind method is used to differentiate equations. The SIMPLE algorithm is also used to solve momentum and energy equations simultaneously.

3. Boundary conditions

3.1. Inlet

The "Mass Flow Inlet" boundary condition was used for the inlet boundary of the vortex tube according to the CFD model used by Skye et al. [20], which is determined by the total mass flow rate, the stagnation temperature, and the direction of the inlet flow vector. According to the experimental results, the boundary conditions in the inlet are almost constant so that the mass flow rate at the inlet and stagnation temperatures are considered as 8.34 g/s and 294.2 K, respectively. The inlet flow vector is considered perpendicular to the inlet boundary.

3.2. Cold exit

The "Pressure Outlet" boundary condition is used in cold exit. In other words, the static pressure is assumed to be known in the cold exit and is fixed and determined based on experimental results [20]. According to experimental results, the pressure is assumed to be very low in the cold exit. In this numerical study, the pressure value has been determined to be 15895 Pa based on experimental results.

Another remarkable note is that in the low mass fraction in the cold exit, the CFD model shows a backflow in the cold air exit. Therefore, the backflow temperature must be determined. Various methods are available to determine the backflow temperature, which can be found in the references. In this numerical study, the results of previous references in this field have been used to calculate the backflow temperature [21,22]. On this basis, the backflow temperature is assumed to be the mean total temperature of the flow leaving the cold exit. In this study, the backflow temperature is considered to be 290 K.

3.3. Hot exit

The "Pressure Outlet" boundary condition has been applied to the hot exit similar to that applied to the cold exit. However, the difference is that the pressure

in the hot exit is assumed to be variable as long as the desired mass ratio is satisfied at the cold exit.

3.4. The vortex tube wall

The "Non-slip" boundary condition has been applied to the solid surfaces. By applying this condition, all velocity components at the walls are zero. These surfaces are considered to be adiabatic. In the shear sections, the periodic boundary condition is used due to the symmetry of flow and geometry. All boundary conditions are shown in Figures 3 and 4.

4. Results

4.1. Grid independency study

To eliminate and reduce any errors due to the coarseness or inappropriate dimensions of the fluid field mesh and the independence of the analysis results from the effects of meshing, numerical modeling was conducted with different mesh sizes to investigate the effect of the number of meshes. The vortex tube model was considered at a cold gas mass ratio of $\alpha = 0.3$, and the key parameters such as temperature separation at the cold exit and swirl velocity in the vortex chamber were considered as comparison criteria. In addition, according to the conducted study, for the volume of elements less than 0.0275 mm^3 (the number of elements more than 160,000), the change in the results is negligible and, thus, has no considerable effect. Therefore, according to the approximate stability of results showing the independence of the analysis results from the meshing effects, the same number of elements was used to reduce the calculation time. Further, to investigate other models that are exposed to changes in the nozzle, elements with a mean volume of the examined model were used to be independent of mesh size. The results are shown in Figures 5 and 6.

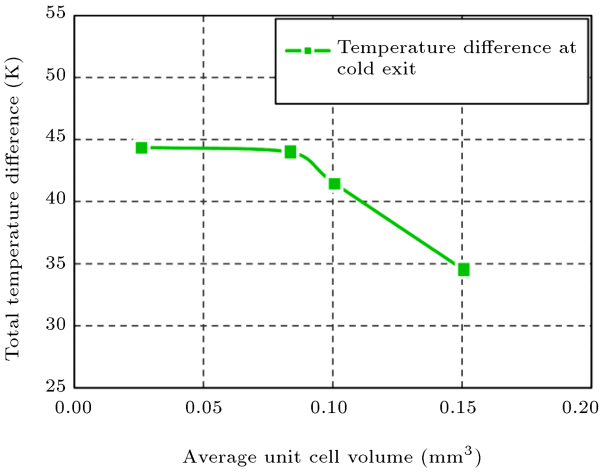

Figure 5. Grid independency study based on maximum cold temperature separation.

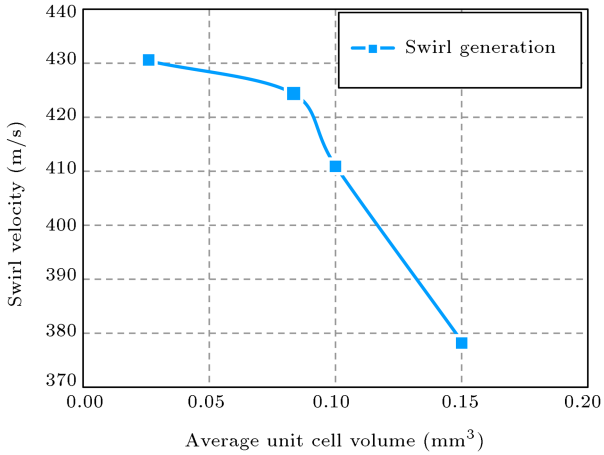

Figure 6. Grid independency study based on maximum swirl velocity in the vortex chamber.

4.2. Examining the turbulence model

As mentioned earlier, the considered model is a rotary 3D model with axial symmetry. $k-\varepsilon$ and $k-\omega$ and SST turbulence models were used to simulate the flow turbulence and investigate the effect of different types of turbulence models on the modeling of energy separation phenomenon of rotating and compressible flow in the vortex tube. In addition, the problem was modeled with other turbulence models such as RNG $k-\varepsilon$ and RSM. The application of these turbulence models for the considered geometry was accompanied by divergence in the soluble field.

The comparison of numerical modeling results shows a good correlation between $k-\varepsilon$ turbulence model and experimental results. The temperature separation obtained at cold and hot exits with different turbulence models was compared with the experimental results of Skye et al. [20] in Figures 7 and 8, respectively. As shown in these figures, the calculated temperature for the hot exit gas (T_h) is in accordance with experimental results in the majority of the turbulence models. However, the results obtained for the

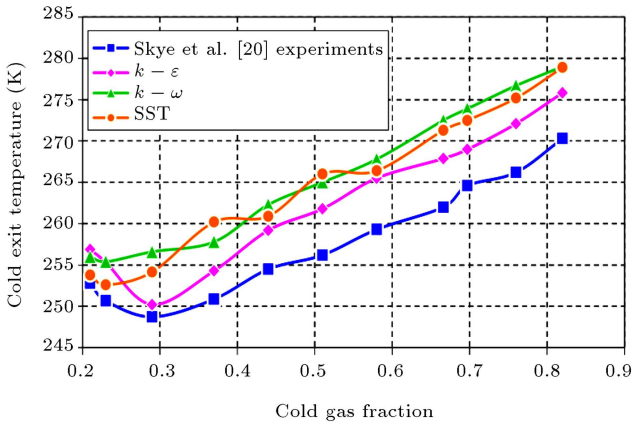

Figure 7. Cold exit gas temperature for different turbulence models.

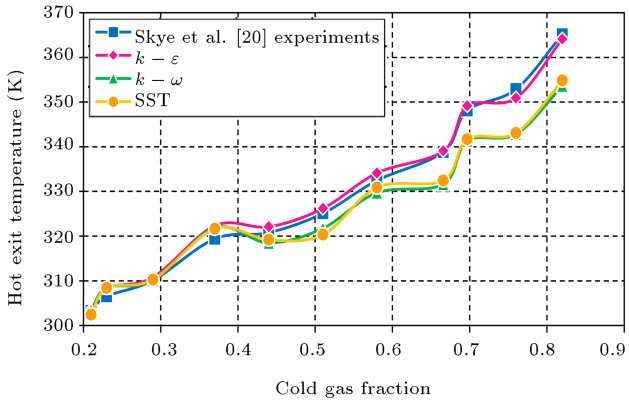

Figure 8. Hot exit gas temperature for different turbulence models.

cold exit gas temperature (T_c) with $k-\varepsilon$ model show the highest accordance with the experimental data.

Therefore, it can be concluded that the $k-\varepsilon$ turbulence model enjoys higher accuracy and ability than other models for the simulation of rotational flow in the vortex tube, and this model can be used for the design and numerical optimization of the vortex tube with high accuracy.

4.3. Validation of numerical results

The numerical model results were compared with the experimental results in [20], and all comparisons between the model and experimental data were reported based on the cold mass fraction.

Figure 9 shows the comparison of temperature separation performances at the cold exit. As can be seen, the temperature separation resulting from the numerical model at the cold exit at the lowest cold mass fraction is about 37°C. By increasing the mass fraction at the cold exit to 0.3, the temperature separation at the cold exit increases to 44°C. Based on this point, an increase in mass fraction at the cold exit is accompanied by a reduction in the temperature separation in this region.

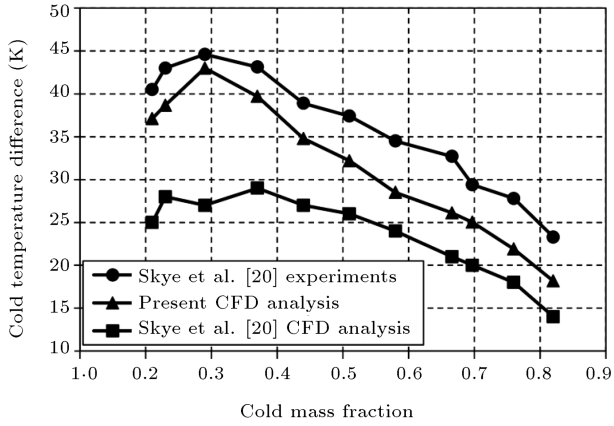

Figure 9. Temperature separation obtained at the cold exit.

In the hot exit region shown in Figure 10, at a cold mass fraction of 0.2, the lowest temperature separation is observed at the hot exit. By increasing the cold mass fraction, the temperature separation in the hot exit region increases with an upward trend so that, in the cold mass fraction of 0.81, the temperature separation at the hot exit increases to 70°C. According to the presented diagrams, acceptable agreement is observed between the 3D model and the existing experimental model, and the maximum error rate is about 10%. It can be seen that the 3D model of the present analysis is better than the two-dimensional model of Skye et al. [20], and its results are closer to experimental results, especially at the cold exit.

4.4. Investigating the effect of inlet pressure on the performance of the vortex tube

In order to investigate the effect of inlet pressure, the performance of the device has been studied in a pressure range of 3.47 to 7.24 bars. It should be noted that the equivalent pressure of the experimental model of Skye et al. [20] is 4.8 bars. Thus, some inlet pressures lower and more than the aforementioned value have been investigated. Figures 11 and 12 show

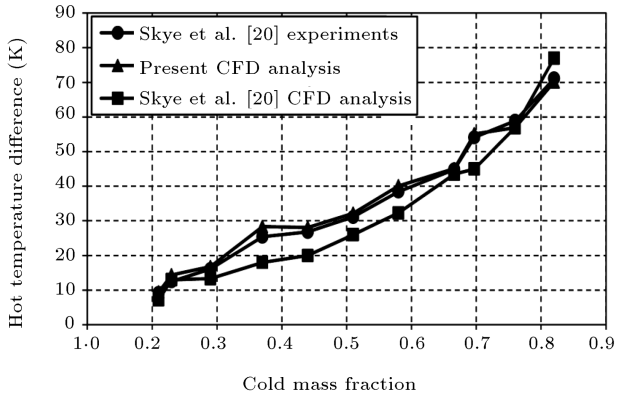

Figure 10. Temperature separation obtained at the hot exit.

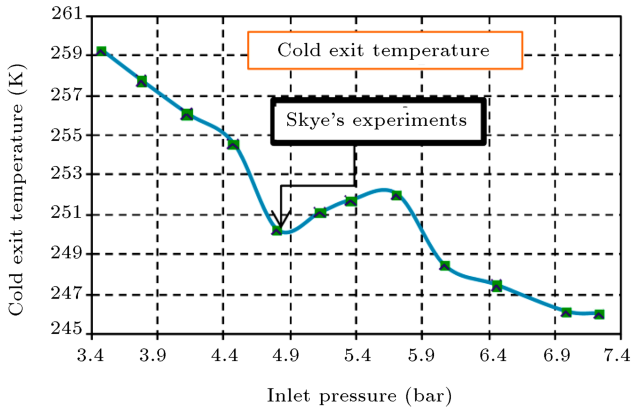

Figure 11. Cold exit temperature for different inlet pressures.

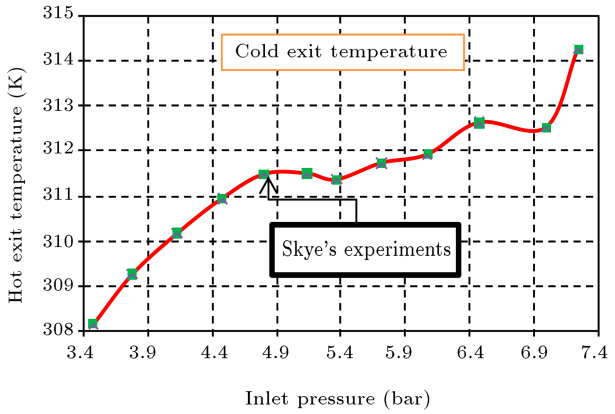

Figure 12. Hot exit temperature for different inlet pressures.

the energy separation at cold and hot exits. The presented results in this section include a mass ratio of 0.3 at the cold exit.

According to Figure 11, at first, the cold exit temperature decreases with an increase in inlet pressure, which is in line with expectations and consistent with the results of previous papers in this field. However, with an increase in inlet pressure in the range of 4.8 to 5.71 bars, the cold exit temperature increases instead of decreasing. However, from 5.71 bars of inlet pressure, an increase in pressure decreases the cold exit temperature and, thus, increases the cooling produced by the vortex tube.

According to Figure 12, the overall trend of hot exit temperature variation in terms of an increase in inlet pressure is ascending. However, there are fluctuations between 5.13 and 7 bars. As mentioned, the vortex tube is used for cooling and not for heating in most industrial applications. Therefore, the temperature behavior of the cold exit is more important than that of the hot exit.

Figure 11 shows that in the range of 3.47 to 5.71 bars, the lowest observed temperature at the cold exit is related to the inlet pressure of 4.8 bars (the pressure associated with the Skye experimental model [20]), which is 250.24 K. Now, if there is a temperature lower than this value, we should increase the pressure to at least 6 bars. It is known that the pressure increase incurs greater costs, which may not be economical. For example, if there is an increase in the inlet pressure by 50% compared to an inlet pressure of 4.8 bars proposed by Skye et al. [20] and about 7.24 bars are reached, only a 4.2 K increase in cooling will be observed, which is not economically justifiable.

Figure 13 shows the total temperature distribution across the tube for a model with an inlet pressure of 4.8 bars. The maximum values for the total temperature are observed near the vortex tube wall due to the non-slip boundary condition. At the central core of the tube, the temperature is lower than that close to the wall. There is a gradual decrease in temperature by moving the fluid flow from the hot exit to the cold one. Moreover, an increase in temperature is observed in the radial direction and toward the vortex tube wall.

The total temperature contour for the vortex tube in a cold mass ratio of 0.3 indicates that the maximum temperature of the hot gas exit is 311.5 K and the minimum cold gas temperature is 250.24 K. Total temperature variations indicate a decrease in the total temperature gradient in regions close to the hot exit.

Pressure variations within the vortex tube lead to changes in the Mach number. Therefore, checking the Mach number inside the field can be effective in understanding the flow, as shown in Figure 14. In this figure, the Mach number variations within the vortex chamber are displayed. This figure shows that the flow in the nozzle inlet is subsonic, but with a high Mach number (about 0.9). As the fluid moves along the nozzle and enters into the vortex chamber, the Mach number increases and the flow becomes supersonic. As the fluid continues to move within the chamber, the Mach number decreases after reaching its maximum value and the flow suddenly becomes subsonic. This indicates the shock occurrence inside

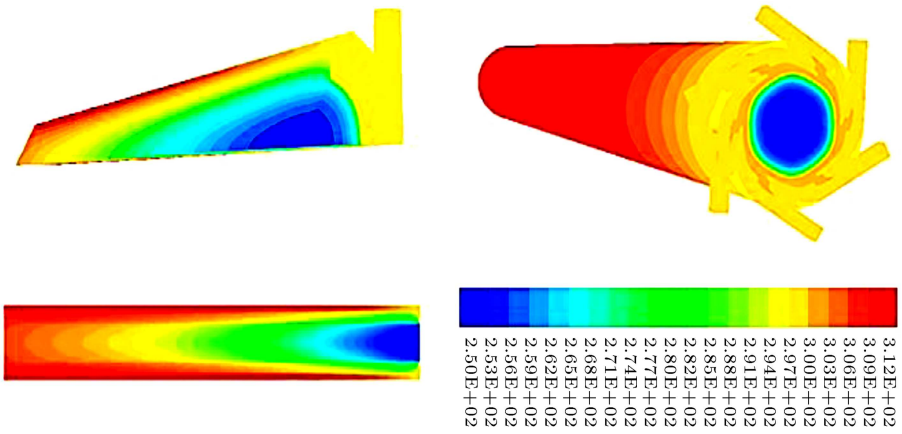

Figure 13. Total temperature distribution throughout the vortex tube.

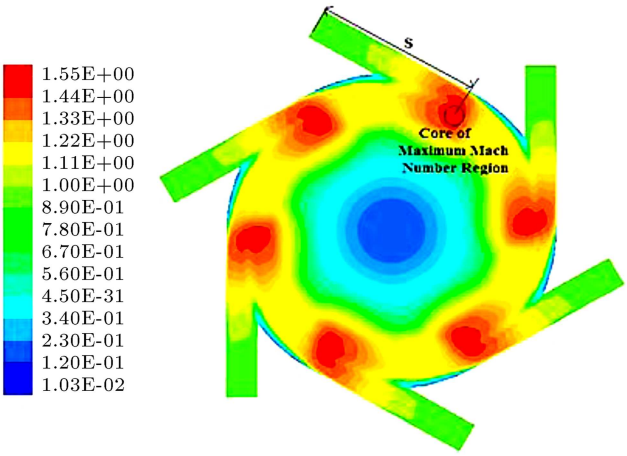

Figure 14. Mach number distribution contours in the vortex chamber.

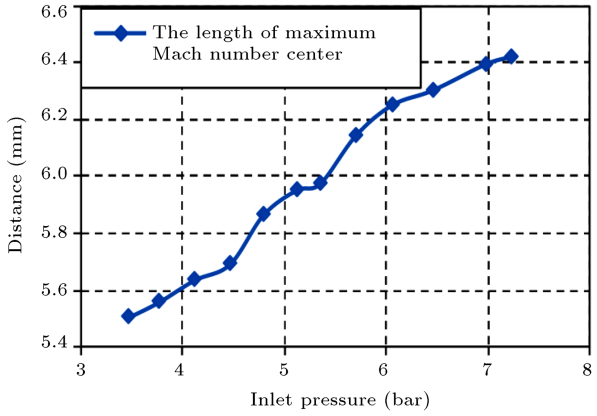

Figure 15. Changes in the distance of center of high pressure core to the nozzle inlet due to increase in inlet pressure.

the vortex chamber, which is accompanied by drops in the system including pressure drops.

If the location of maximum Mach number (Figure 14) is considered as a core with a high Mach number and the distance is shown from the center of this core to the nozzle inlet with S, the results of this study show that an increase in inlet pressure leads to a gradual increase in the distance S; in this way, the high pressure core is kept out of the nozzle and moves towards the outlet of the next nozzle. These changes are shown in Figure 15. Figure 16 shows the Mach number variations in the radial direction in the vortex chamber. It is evident from this figure that the radial moving from the center increases the Mach number due to an increase in r and, subsequently, an increase in axial velocity.

Through the calculated velocity field, the path lines for fluid elements in the cold mass fraction of 0.3 in 3D coordinates are shown in Figure 17. Fluid elements evacuated from the cold exit progress with a rotating motion towards the end of the vortex tube.

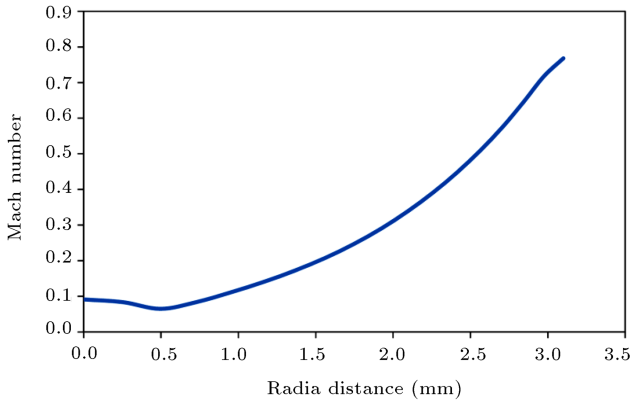

Figure 16. Mach number variations along the radial line passing through the vortex chamber.

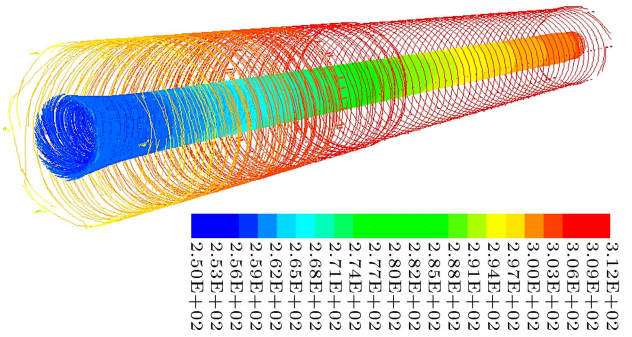

Figure 17. Path lines for fluid within the vortex tube in terms of total temperature.

A part of fluid element moves to the cold exit along the initial length of the vortex tube, and other fluid elements move to the end of the hot exit of vortex tube and change their direction near the end of the tube and start moving towards the cold exit, while their rotating motion decreases during this path. Another part of fluid elements flows toward the hot exit with a rotating motion after entering the peripheral region of the vortex tube. It can be seen that the interaction of the flow at hot and cold exits occurs at a distance before the hot exit. Therefore, the major energy separation is generated before reaching this point. According to the obtained path lines, it is clear that, at low mass fraction at the cold exit, the return of flow to the cold exit takes place near the hot exit of tube.

4.5. Investigating the second law of thermodynamics for the vortex tube

According to the Clausius statement of the second law of thermodynamics, heat transfer from a cold source to a hot source is impossible without external work being performed on the system. On the other hand, as mentioned before, the vortex tube has no input work, and a question arises as to whether this device can satisfy the second law of thermodynamics. To analyze this subject, considering $\dot{m}_i$, $\dot{m}_c$, and $\dot{m}_h$ as the inlet air, the cold, and the hot exit mass flow rates,

respectively, and based on the law of conservation of mass, the following is obtained:

$$\dot{m}_i = \dot{m}_c + \dot{m}_h. \tag{1}$$

Since there is no input or output heat transfer and work, the first thermodynamic law for the system is written as follows:

$$(\dot{m}_c + \dot{m}_h)h_i = \dot{m}_c h_c + \dot{m}_h h_h. \tag{2}$$

Since the air has been considered as an ideal gas from the beginning, Eq. (3) is as follows:

$$(\dot{m}_c + \dot{m}_h)T_i = \dot{m}_c T_c + \dot{m}_h T_h, \tag{3}$$

where T_i, T_c, and T_h are the inlet air, the cold exit, and the hot exit temperatures, respectively. According to the definition of α in Eq. (4) and placement in Eq. (5) we have the following:

$$\alpha = \frac{\dot{m}_c}{\dot{m}_{in}}, \tag{4}$$

$$T_i = \alpha T_c + (1-\alpha)T_h. \tag{5}$$

Entropy changes during the process are calculated through the following equation:

$$\Delta S = \dot{m}_c s_c + \dot{m}_h s_h - \dot{m}_i s_i$$

$$= \dot{m}_c(s_c - s_i) + \dot{m}_h(s_h - s_i). \tag{6}$$

Assuming the air as an ideal gas, we have the following equations:

$$s_c - s_i = c_p \ln(\frac{T_c}{T_i}) - R\ln(\frac{P_c}{P_i}), \tag{7}$$

$$s_h - s_i = c_p \ln(\frac{T_h}{T_i}) - R\ln(\frac{P_h}{P_i}), \tag{8}$$

where P_i, P_c, and P_h are the inlet air, the cold exit, and the hot exit pressures, respectively. Eq. (13) can be rewritten as follows:

$$\Delta s = \frac{\Delta \dot{S}}{\dot{m}_i} = \alpha\left[c_p \ln\left(\frac{T_c}{T_i}\right) - R\ln\left(\frac{P_c}{P_i}\right)\right]$$

$$+ (1-\alpha)\left[c_p \ln\left(\frac{T_h}{T_i}\right) - R\ln\left(\frac{P_h}{P_i}\right)\right]. \tag{9}$$

It is known here that the air of vortex tube exits into the environment; thus, $P_h = P_c = P_a$ and Eq. (16) can be rewritten as follows:

$$\Delta s = c_p\left\{\ln\left[\left(\frac{T_c}{T_i}\right)^{\alpha}\left(\frac{T_h}{T_i}\right)^{1-\alpha}\right]\right.$$

$$\left. - R\ln\left[\left(\frac{P_a}{P_i}\right)^{\frac{k-1}{k}}\right]\right\}, \tag{10}$$

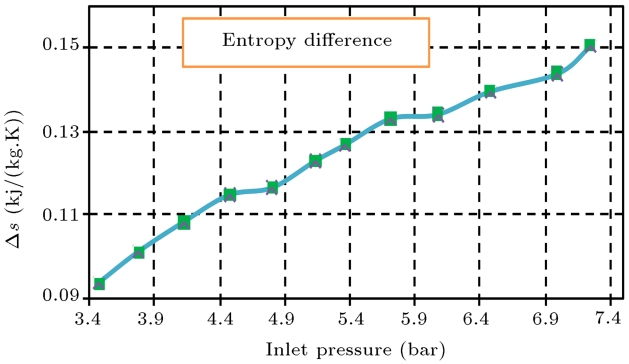

Figure 18. The created entropy difference in terms of various inlet pressures of the vortex tube.

where C_p and k have constant values of 1.004 and 1.4, respectively. By inserting these values, for different values of cold and hot exit temperatures and inlet pressures, the values of Δ_s are obtained according to Figure 18. The figure shows that for all different inlet pressures, all values of Δ_s are positive and greater than zero. It means that the second law of thermodynamics for vortex tube is true and not violated. Figure 15 also shows that an increase in inlet pressure increases the entropy production and, subsequently, the system disorder.

5. Conclusion

In this study, Fluent software and finite volume method were used to model the energy separation phenomenon in the vortex tube. The purpose of this paper was to study the effect of inlet pressure parameter. The numerical solution was validated based on experimental results. Investigations were carried out to find the optimal inlet pressure to reduce the cold exit temperature (increase in cooling amount) and increase the hot exit temperature (increase in heating amount). The results showed that the proper inlet pressure increased the cooling and heating amounts and, also, reduced the costs. For the studied vortex tube in this paper, it is recommended that 4.8 bars of inlet pressure be used. The Mach number investigation in the vortex chamber is also a confirmation of the occurrence of shock impact wave phenomenon in this part of the vortex tube device. The occurrence of this phenomenon causes losses and irreversible changes in the system, which can be reduced by strategies. As pressure increases, the high pressure core deviates from the nozzle and moves towards the outlet of the next nozzle. The cold flow mass ratio is the key parameter in controlling the temperature of cold and hot exits. An increase in inlet pressure increases the entropy production and, subsequently, causes system disorder. For cooling purposes, the use of cold mass fraction of about 0.3 would result in a higher separation in the cold exit and,

for heating purposes, a cold mass ratio of about 0.8 is recommended. The present obtained results showed that the maximum exergy efficiency occurs at $\alpha = 0.21$. In addition, the maximum and minimum exergy loss occur at $\alpha = 0.3691$ and $\alpha = 0.21$, respectively.

References

1. Pourmahmoud, N., Sepehrian Azar, F., and Hassanzadeh, A. "Numerical simulation of secondary vortex chamber effect on the cooling capacity enhancement of vortex tube", *Heat Mass Transfer*, **50**(9), pp. 1225–1236 (2014).
2. Pourmahmoud, N., Esmaily, R. and Hassanzadeh, A. "Experimental investigation of diameter of cold end orifice effect in vortex tube", *J. of Thermophys. and Heat Transfer*, **29**(3), pp. 629–633 (2015).
3. Ghafouri, A. and Hassanzadeh, A. "Numerical simulation of motion and deformation of healthy and sick red blood cell through a constricted vessel using hybrid lattice Boltzmann-immersed boundary method", *J. the Brazilian Soc. of Mech. Sci. and Eng.*, **39**(6), pp. 1873–1882 (2017).
4. Pourmahmoud, N., Jahangiramini, A., Hassanzadeh A., and Izady, A. "Numerical investigation of energy separation in a low pressure vortex tube under different axial angles of injection nozzles", *Modarres Tech. and Eng. Sci. Res. J.*, **13**(7), pp. 64–73 (2013) (In Persian).
5. Khodayari Bavil, A. and Razavi, S.E. "On the thermo flow behavior in a rectangular channel with skewed circular ribs", *Mech. & Ind.*, **18**(2), p. 225 (2017).
6. Khosravi, M., Mosaddeghi, F., Oveisi, M., and Khodayari Bavil, A. "Aerodynamic drag reduction of heavy vehicles using append devices by CFD analysis", *J. Cent. South Univ.*, **22**, pp. 4645–4652 (2015).
7. Mohammadi, B., Rohanifar, M., Salimi-Majd, D., and Farrokhabadi, A. "Micromechanical prediction of damage due to transverse ply cracking under fatigue loading in composite laminates", *J. Reinforced Plast. and Compos.*, **36**(5), pp. 377–395 (2017).
8. Pourmahmoud, N., Hassanzadeh, A., Motaby, O., and Bramo, A. "Computational fluid dynamics analysis of helical nozzles effect on the energy separation in a vortex tube", *Therm. Sci.*, **16**(1), pp. 151–166 (2012).
9. Ranque, G.J. "Experiences sur la détente giratoire avec simultanes d'un echappement d'air chaud et d'un enchappement d'air froid", *J. Phys. Radium*, **4**, pp. 112–114 (1933).
10. Hilsch, R. "Die expansion von gasen im zentrifugalfeld als kälteproze", *Z. Naturforschung*, **1**, pp. 208–214 (1946).
11. Khazaei, H., Teymourtash, A.R., and Malek-Jafarian, M. "Effects of gas properties and geometrical parameters on performance of a vortex tube", *Scientia Iranica*, **19**(3), pp. 454–462 (2012).
12. Dawoodian, M., Dadvand, A., and Hassanzadeh, A. "A numerical and experimental study of the aerodynamics and stability of a horizontal parachute", *ISRN Aerospace Engineering*, Article ID 320563, **2013**, 8 pages (2013).
13. Pourmahmoud, N., Rafiee, E., Rahimi, M., and Hassanzadeh, A. "Numerical energy separation analysis on the commercial Ranque-Hilsch vortex tube on basis of application of different gases", *Scientia Iranica*, **20**(5), pp. 1528–1537 (2013).
14. Behera, U., Paul, P.J., Kasthurirengen, S., Karunanithi, R., Ram, S.N., Dinesh, K., and Jacob, S. "CFD analysis and experimental investigations towards optimizing the parameters of Ranque-Hilsch vortex tube", *Int. J. Heat Mass Transfer*, **48**, pp. 1961–1973 (2005).
15. Shamsoddini, R. and Hossein Nezhad, A. "Numerical analysis of the effects of nozzles number on the flow and power of cooling of a vortex tube", *Int. J. Refrigeration*, **33**, pp. 774–782 (2010).
16. Pourmahmoud, N., Izady, A., Hassanzadeh, A., and Jahangiramini, A. "Computational fluid dynamics analysis of the influence of injection nozzle lateral outflow on the performance of Ranque-Hilsch vortex tube", *Therm. Sci.*, **18**(4), pp. 1191–1201, (2014).
17. Pourmahmoud, N., Esmaily, R., and Hassanzadeh, A. "CFD investigation of vortex tube length effects as a designing criterion", *Int. J. of Heat and Tech.*, **32**(1), pp. 129–136 (2015).
18. Ameri, M. and Behnia, B. "The study of key design parameters effects on the vortex tube performance", *J. Therm. Sci.*, **4**, pp. 370–376 (2009).
19. Zhidkov, M.A., Komarova, G.A., Gusev, A.P., and Iskhakov, R.M. "Interrelation between the separation and thermodynamic characteristics of three-flow vortex tubes", *Chem. Petro. Eng.*, **37**, pp. 271–277 (2001).
20. Skye, H.M., Nellis G.F., and Klein, S.A. "Comparison of CFD analysis to empirical data in a commercial vortex tube", *Int. J. Refrig.*, **29**, pp. 71–80 (2006).
21. Pourmahmoud, N., Rashidzadeh, M., and Hassanzadeh, A. "CFD investigation of inlet pressure effects on the energy separation in a vortex tube with convergent nozzles", *Eng. Comput.*, **32**(5), pp. 1323–1342 (2015).
22. Pourmahmoud, N., Izadi, A., Hassanzadeh, A., and Jahangiramini, A. "Computational fluid dynamics analysis of the influence of injection nozzle lateral outflow on the performance of Ranque-Hilsch vortex tube", *Therm. Sci.*, **18**(4), pp. 1191–1201 (2014).

Biographies

Nader Pourmahmoud was born in 1969 in Iran. He received his BS degree in Mechanical Engineering from Shiraz University in 1992. After achieving some

practical engineering projects till 1997, he started his MSc degree in Mechanical Engineering (energy conversion field) in Tarbiat Modarres University in Tehran and, finally, he received his PhD degree in Mechanical Engineering (energy conversion field) in 2003 at the same university. He has joined the Faculty of Engineering of Urmia University since 2003, where he is a Professor at the Mechanical Engineering Department. His professional interest is in the field of CFD of turbulent fluid flows, energy conversion problems especially in the energy exchangers.

Omid Moutaby was born in 1985 in Iran. He received BS degree in Mechanical Engineering from Islamic Azad University of Tabriz in 2008. He received MSc degree in Mechanical Engineering (energy conversion field) from Urmia University in Iran in 2012. Currently, he is a PhD student at Urmia University. His main research favorites include CFD, energy conversion, and vortex tube.